

Analysis of pool boiling heat transfer over porous surfaces

S. Madhusudana Rao, A. R. Balakrishnan

463

Abstract A semi-empirical model for pool boiling over porous surfaces is presented. The pressure drop across the porous surface is estimated using Darcy's law. The significance of the latent heat flux contribution for highly porous surfaces is examined. Two nucleation factors are defined and correlated in terms of measurable quantities using literature data. An expression for the total heat flux in terms of the wall superheat, pore geometry and the physical properties of the liquid is presented. The present model matches well with literature data on pool boiling over porous surfaces, both flat surfaces and tubes from four different sources, thus validating the present approach.

Untersuchung des Wärmeübergangs beim Behältersieden über porösen Oberflächen

Zusammenfassung Vorgestellt wird ein halbempirisches Modell für das Behältersieden über porösen Oberflächen. Die Berechnung des Druckabfalls in der porösen Schicht erfolgt gemäß dem Gesetz von Darcy. Der Einfluß des Latentwärmeflusses bei hochporösen Oberflächen wird untersucht. Unter Verwendung von Daten aus der Literatur werden die für die Keimbildung wichtigen Faktoren definiert und zu meßbaren Größen in Beziehung gesetzt. Für den Gesamtwärmefluß läßt sich ein Ausdruck finden, der diesen in Abhängigkeit von Wandüberhitzung, Porengeometrie und den physikalischen Eigenschaften der Flüssigkeit bestimmt. Das vorgestellte Modell liefert Ergebnisse, die gut mit aus vier Quellen entnommenen Literaturdaten bezüglich Behältersieden über porösen Oberflächen übereinstimmen, und zwar sowohl für ebene Oberflächen wie auch für Rohre.

List of symbols

C_p	specific heat, J/(kg K)
d	diameter of the pore, m
d_p	diameter of the particle in the porous matrix, m
g	acceleration due to gravity, m/s ²
Ja	Jakob number $- [(\rho_l C_p \Delta T) / (\rho_v \lambda)]$, (-)
K	permeability of the porous matrix, m ²
k	thermal conductivity, W/(m K)
N/A	nucleation site density, 1/m ²
ΔP	pressure drop across the porous matrix defined by Eq. (1), N/m ²
ΔP_{eq}	equilibrium pressure drop defined by Eq. (11), N/m ²
q	total heat flux, W/m ²
q_{ex}	heat flux due to single phase convection, W/m ²
q_l	heat flux due to latent heat contribution, W/m ²
r	pore radius, m
T	temperature, K
ΔT	wall superheat ($= T_w - T_s$), K
U_D	Darcy velocity, m/s

Greek symbols

α	nucleation factor defined by Eq. (17), (-)
β	nucleation factor defined by Eq. (14), (-)
δ	thickness of the porous surface, m
ϵ	porosity of the porous matrix, (-)
λ	latent heat of vaporisation, J/kg
μ	viscosity, N S/m ²
ρ	density, kg/m ³
σ	surface tension, N/m

Subscripts

cri	critical
l	liquid
max	maximum
s	saturated
v	vapour
w	wall

1

Introduction

Enhancement of pool boiling heat transfer is an active area of research and development because of its academic and industrial importance. In recent years, several enhancement techniques for boiling under different operating conditions have been developed and tested. Some of these are GEWA-T surface (Wieland Werke AG, Germany), ECR-40 (Furukuwa Metals Co., Japan) and High Flux surface (Union Carbide, USA). These boiling surfaces are

Received on 11 July 1996

S. Madhusudana Rao
A. R. Balakrishnan
Department of Chemical Engineering
Indian Institute of Technology Madras
Madras 600 036, India

Correspondence to: A. R. Balakrishnan

This work was carried out with financial support from the Department of Atomic Energy, Government of India through the Board of Research in Nuclear Sciences, Bhabha Atomic Research Centre, Mumbai, India.

porous and the cavities in the matrix act as continuous stable nucleation sites. The porous surfaces are made up of metal particles and are produced by either plasma spraying or by sintering. The advantage of using these surfaces is the reduction in the wall superheat (also called the excess temperature) by several times at a particular heat flux and an increase in the critical heat flux by two to three times when compared to a plain surface. There are many studies on boiling on porous surfaces and these have been reviewed by Thome [1], Stephan [2] and Webb [3]. O'Neill et al. [4] developed an analytical model for the boiling over porous surfaces to predict the heat flux. Webb [5] further analyzed the model, which consists of geometric parameters that depends mainly on the particle packing arrangement. These geometric parameters are estimated from expressions developed for regular packings and are approximated for actual packings. Kovalev [6, 7] modelled the heat transfer mechanism within the porous structure using the momentum and energy equations for the liquid and vapour flow within the capillaries. The momentum and energy equations must be numerically solved over the matrix thickness. While the model compared well with their data on water boiling at one atmosphere on a 1.0 mm thick porous matrix made of 0.3–0.4 mm diameter particles, the model has not been compared with other data available in the literature. As Webb [5] states, this is possibly due to the fact that the model is quite complicated to use.

Nakayama et al. [8, 9] while studying boiling over porous surfaces concluded that the phenomenon is highly dynamic. They analyzed the boiling heat transfer on a porous surface that was modelled as a series of interconnected cavities and openings through which the cavities are in contact with the liquid outside the matrix. The internal cavities are a row of tunnels which run under the matrix surface. Their model is based on the “suction-evaporation” mode. The major disadvantage with the model is that it contains several empirical constants that have to be evaluated for different surface and liquid combinations.

Nishikawa et al. [10] proposed an empirical correlation based on their experiments on boiling of R-11, R-113 and benzene at 1.0 atmosphere on porous matrices made of copper and bronze particles of size $0.1 < d_p < 1.0$ mm. Zhang and Zhang [11] conducted experiments on twelve different bronze sintered coatings on a flat surface with particle size in the range $0.11 \leq d_p \leq 0.53$ mm and matrix thickness $0.94 \leq \delta \leq 4.6$ mm using water, ethyl alcohol and R-113 at approximately 100 kPa. Bergles and Chyu [12] experimentally studied the pool boiling of water from a commercial porous metal matrix which provided a basis for the mechanisms they postulated. Afgan et al. [13] experimentally investigated the heat transfer during the boiling of water, ethyl alcohol and R-113 from porous layers with a void fraction of 0.3 to 0.7 at atmospheric pressures. The boiling curves obtained had different shapes depending on the mode of operation, namely, bubble mode, transition mode and film formation (which they called mode II). However, no criteria to establish which mode of boiling occurs has been suggested. Tehver et al. [14] performed experiments on pool boiling over

plasma sprayed coatings. Experimental boiling curves and burn out heat flux data were obtained for nucleate boiling of R-113 on a horizontal surface coated with porous aluminium, bronze, copper and corundum particles.

While a fair amount of experimental data on boiling on porous surfaces have been reported in the literature as can be seen from the brief review above, the various correlations available are specific only to the particular systems from which they were developed, that is the porous coating and the liquid being boiled, and cannot be safely extrapolated to other systems. The present study focuses on the development of an analytical model incorporating bubble dynamics for boiling over porous surfaces. The model is compared with literature experimental data from a wide range of sources in order to validate the approach.

2 The Model

In the development of the model, the following assumptions are invoked:

1. The porous matrix consists of particles of uniform diameter and interconnected so that liquid or vapour can flow between them as illustrated in Fig. 1.
2. The temperature of the porous matrix is constant over its thickness.
3. All the pores on the surface are active at the burnout heat flux which depends only on the geometry of the surface.
4. The liquid being boiled is at its saturation temperature.
5. Coalescence of the bubbles is not considered.

A small superheat is sufficient to initiate nucleation over porous surfaces. The vapour formed in the pores starts moving up as more and more vapour accumulates inside the porous surface. The pressure drop across the porous

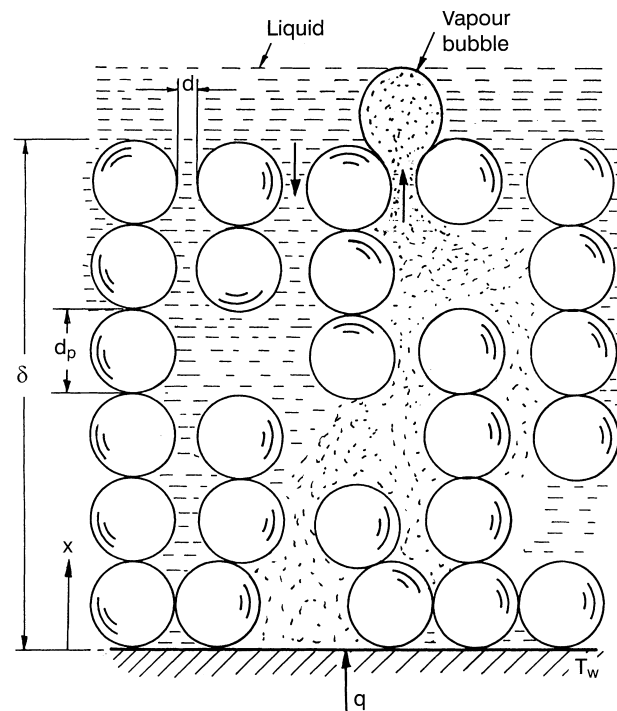


Fig. 1. Model for a porous boiling surface

layer due to the upward movement of the vapour can be estimated using Darcy's law

$$\frac{\Delta P}{\Delta x} = \frac{\mu_v}{K} U_D \quad (1)$$

Assuming the vapour in the porous medium is moving upwards through capillary tubes of diameter 'd' formed between spherical particles of uniform diameter 'd_p', the Darcy velocity 'U_D' can be written as

$$U_D = \frac{\dot{m}}{\rho_v(\pi d^2/4)} \quad (2)$$

where \dot{m} is the mass flow rate of the vapour through the porous layer and is given by

$$\dot{m} = \frac{q_l}{\lambda(N/A)} \quad (3)$$

In the above equation 'q_l' is the latent heat contribution of the total heat flux and (N/A) is the number of active pores per unit area. Substituting Eqs. (2) and (3) into Eq. (1) gives the pressure drop across the porous layer of thickness 'δ'

$$\Delta P = \frac{1.27 q_l \delta \mu_v}{\rho_v \lambda d^2 (N/A) K} \quad (4)$$

The permeability 'K' of the matrix can be evaluated from the straight tube model [15]

$$K = \frac{\epsilon d^2}{32} \quad (5)$$

The latent heat flux can be expressed in terms of the wall superheat (ΔT) if the actual pressure drop across the porous matrix can be substituted into the Clayperon equation

$$\frac{dp}{dT} = \frac{\lambda}{T_s V_{lv}} \quad (6)$$

Using Eq. (4) in Eq. (6) and assuming ΔP = dp

$$q_l = \frac{\rho_l \rho_v^2 K \lambda^2 d^2 (\Delta T) (N/A)}{1.27 \mu_v \delta T_s (\rho_l - \rho_v)} \quad (7)$$

The contribution of the heat flux due to the external convection over the porous surface can be evaluated from an expression due to Nakayama et al. [8]

$$q_{ex} = \left(\frac{\Delta T}{C_q} \right)^{5/3} (N/A)^{1/3} \quad (8)$$

where C_q is an empirical constant which depends on the boiling liquid. For R-11, C_q is 1.95 [K (cm²/W)^{3/5} (1/cm²)^{1/5}]. The expression for the total heat flux is given by

$$q = q_l + q_{ex} \quad (9)$$

The performance of the present model is examined by comparing the experimental data of Nakayama et al. [8] for the two surfaces they worked on, namely R(11)-1 and R(11)-3. Nakayama et al. [8] characterized their porous surfaces in terms of the longitudinal, X₀ and transverse pitch, X_t of the pores. The geometry details of these two surfaces are shown in Table 1. The porosity of the surface

Table 1. Surface geometry of the porous surfaces used by Nakayama et al. [8]

Liquid	Surface number	d × 10 ³ m	X ₀ × 10 ³ m	X _t × 10 ³ m
R-11	R(11)-1	0.10	0.7	0.55
	R(11)-3	0.04	0.7	0.55

is assumed to be equal to the fraction of the surface free area and can be expressed by

$$\epsilon = \frac{\pi d^2}{4 X_0 X_t} \quad (10)$$

Comparison of the present model with the data of Nakayama et al. [8] is shown in Fig. 2 and the close agreement between the two is apparent.

Figure 3 shows the comparison of the present model with the 'dynamic' model of Nakayama et al. [9]. From the figure it can be seen that the present model is as good as if not better than the Nakayama et al. [9] model. Furthermore, as stated earlier, the Nakayama et al. [9] model is a little unwieldy to use as it has seven empirical constants. The present model based on Darcy's law has only one empirical constant.

The present model can also be used to predict the number of active nucleation sites at any heat flux for a given surface geometry, i.e. given ε the permeability can be evaluated using Eq. (5) and (N/A) can be evaluated using Eq. (7). Figure 4 shows the (N/A) values predicted by the present model against the heat flux for the R(11)-1 surface and is compared with the experimental data and the model of Nakayama et al. [9]. Additional data on (N/A) values

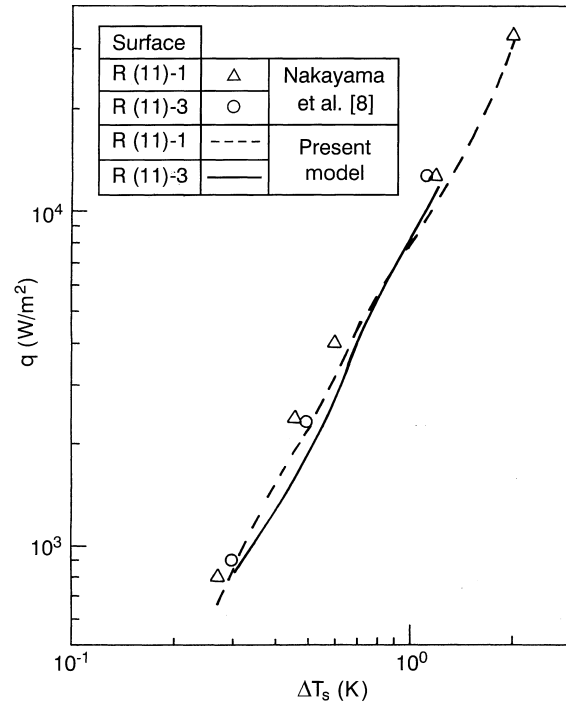


Fig. 2. Comparison of the present model with data of Nakayama et al. [8]

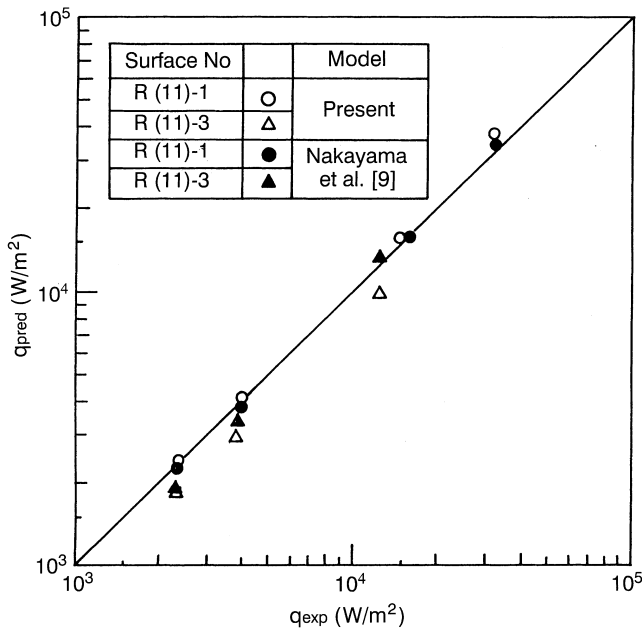


Fig. 3. Comparison of the present model with the model of Nakayama et al. [9]

for porous surfaces are not easily available in the literature. It is for this reason, comparison of the present model is restricted to the data of Nakayama et al. [8].

3 Discussion

The equilibrium condition for a bubble to exit from a cavity of radius r is given by the Thompson equation (sometimes referred to as the Gibbs equation)

$$\Delta P_{eq} = \frac{2\sigma}{r} \tag{11}$$

where σ is the surface tension of the liquid. In porous surfaces, the upward movement of the vapour causes a pressure gradient across the matrix. When the vapour

reaches the surface, if equilibrium conditions exist, then the vapour bubble will easily detach from the pore. Equation (4) shows that ΔP is dependant on q_l . At low heat fluxes, when ΔP is less than the equilibrium pressure drop, the bubble has to wait at the pore mouth until equilibrium conditions are reached before it can detach and rise. At this point the true ΔP will be equal to ΔP_{eq} . Therefore, in general, the dP value in Clayperon's equation should be the larger of ΔP_{eq} and ΔP .

Figure 5 shows the ratio of ΔP obtained from Eq. (4) (which is a function of q_l) and ΔP_{eq} against the total heat flux for each of the two surfaces used by Nakayama et al. [8]. It can be seen that for R(11)-1 surface, when the heat flux is greater than $1.3 \times 10^3 \text{ W/m}^2$, the ratio ($\Delta P/\Delta P_{eq}$) is larger than one. For the R(11)-3 surface, the ratio ($\Delta P/\Delta P_{eq}$) is greater than one for heat flux values above $6 \times 10^3 \text{ W/m}^2$. When ($\Delta P/\Delta P_{eq}$) is greater than one, equilibrium conditions are met before the vapour reaches the mouth of the pore and the bubble can easily detach from the surface. At these heat fluxes there is a free flow of vapour from the surface to the bulk of the liquid.

The contributions of the latent heat flux and the convective heat flux to the total heat flux can be evaluated from Eqs. (7) and (8). The latent heat contribution for the R(11)-1 surface is nearly 40% of the total heat flux. On the other hand the latent heat flux is negligible for the R(11)-3 surface. Since the major contribution for the R(11)-3 surface is from the convective heat flux, the present model is able to predict with sufficient precision heat flux values even when they are less than $6 \times 10^3 \text{ W/m}^2$.

The void fraction, ϵ estimated by Eq. (10) are 0.02 and 0.013 for R(11)-1 and R(11)-3 surfaces respectively. The corresponding (N/A) values will be low since ϵ is low. The void fraction of porous surfaces reported elsewhere in the literature is of a much higher order compared to the surfaces in the Nakayama et al. [8] study. It is believed that the additive mechanism suggested by Nakayama et al. [8] is closer to that of plain surfaces. Generally porous surfaces are known for very high nucleation site densities. On

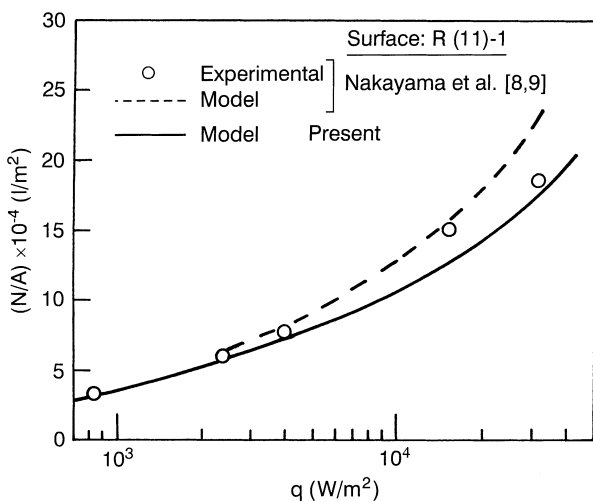


Fig. 4. Comparison of model and experimental data of Nakayama et al. [8] on nucleation site density

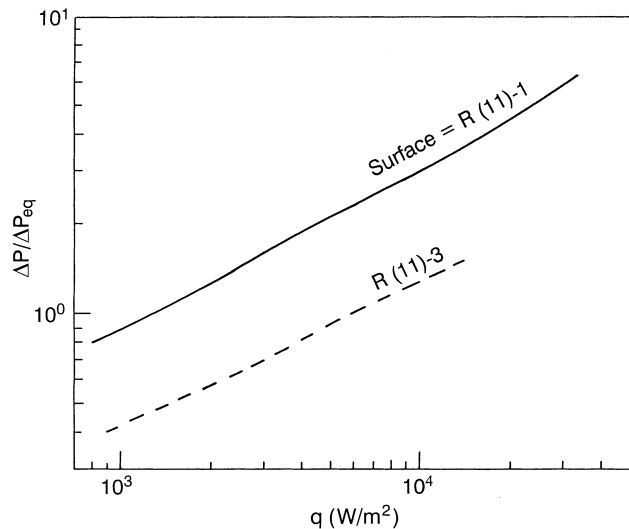


Fig. 5. Pressure ratio against heat flux for two surfaces reported by Nakayama et al. [8]

the basis of their experimental studies, they found that the contribution to the heat flux due to external convection was 10% of the total. However, Eq. (8) which is also due to Nakayama et al. [8] shows that the external heat flux is proportional to the one third power of (N/A) . This means that the porous surfaces with a high porosity and hence large (N/A) values will give rise to an external convection using the Nakayama et al. [9] approach that is much higher than the 10% reported experimentally by them. It is therefore believed that for highly porous surfaces, the total heat flux is removed mostly as latent heat and the convective heat flux can be ignored.

In view of the above, the total heat flux for porous surfaces can be estimated by modifying Eq. (7) by substituting q for q_l

$$q = \frac{\rho_l \rho_v^2 K \lambda^2 d^2 (N/A) \Delta T}{1.27 \mu_v \delta T_s (\rho_l - \rho_v)} \quad (12)$$

To use this expression, (N/A) values are required. Since this information is not easily available in the literature, the model can be modified into a more useful form as follows:

Figure 6 shows an idealized arrangement of the spherical particles in the porous medium (face centred cubic) with uniform diameter ' d_p ' giving rise to maximum number of pores of diameter ' d '. The maximum (N/A) for this ideal geometry is

$$(N/A)_{\max} = \frac{1}{18.1 d^2} \quad (13)$$

A factor ' β ' which is only a function of the geometrical properties of the porous matrix is defined as

$$\beta = \frac{(N/A)_{\text{cri}}}{(N/A)_{\max}} \quad (14)$$

As stated earlier, at burnout all the pores in a porous medium are active and this gives rise to $(N/A)_{\text{cri}}$. The factor ' β ' gives a measure of the deviation of an actual porous matrix to an ideal one. The $(N/A)_{\text{cri}}$ values can be evaluated using Eq. (12) with the burnout data of Tehver et al. [14] for various porous surfaces. ' β ' can now be determined using $(N/A)_{\text{cri}}$ and $(N/A)_{\max}$ in Eq. (14) and correlated with the geometrical characteristics of the porous surface, namely δ (thickness of the porous matrix), d (pore diameter) and ϵ (void fraction of the matrix) as

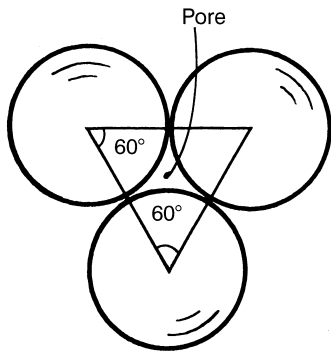


Fig. 6. Arrangement of spherical particles for an ideal porous matrix

$$\beta = \frac{7.41 \times 10^{-3} \left(\frac{\delta}{d}\right)^{0.8}}{\epsilon^{1.31}} \quad (15)$$

The performance of the above correlation with reference to the data of Tehver et al. [14] is shown in Fig. 7. $(N/A)_{\text{cri}}$ can also be expressed in terms of the pore geometry

$$(N/A)_{\text{cri}} = \frac{4.1 \times 10^{-4} \left(\frac{\delta}{d}\right)^{0.8}}{\epsilon^{1.31} d^2} \quad (16)$$

Tehver et al. [14] have also reported a large amount of data for different heat flux values below the burnout heat flux. The (N/A) values at any heat flux below the burnout heat flux will be less than the $(N/A)_{\text{cri}}$ value. Another factor ' α ' is defined as

$$\alpha = \frac{(N/A)}{(N/A)_{\text{cri}}} \quad (17)$$

where $\alpha \leq 1$. The α values at different heat fluxes are evaluated for different porous matrices using the experimental data of Tehver et al. [14]. The α values so obtained are correlated in terms of the Jakob number and the nucleation factor β

$$\alpha = \frac{0.54 (Ja)^{0.22}}{\beta^{0.06}} \quad (18)$$

A very large number of α values obtained from the data of Tehver et al. [14] match the above expression very well and the performance of the correlation is shown in Fig. 8.

Combining Eqs. (15)–(18), (N/A) can be written as

$$N/A = \frac{3 \times 10^{-4} \left(\frac{\delta}{d}\right)^{0.8} (Ja)^{0.22}}{\epsilon^{1.23} d^2} \quad (19)$$

Substituting the above expression for (N/A) into Eq. (12) gives a simple explicit equation for the boiling heat flux in porous media.

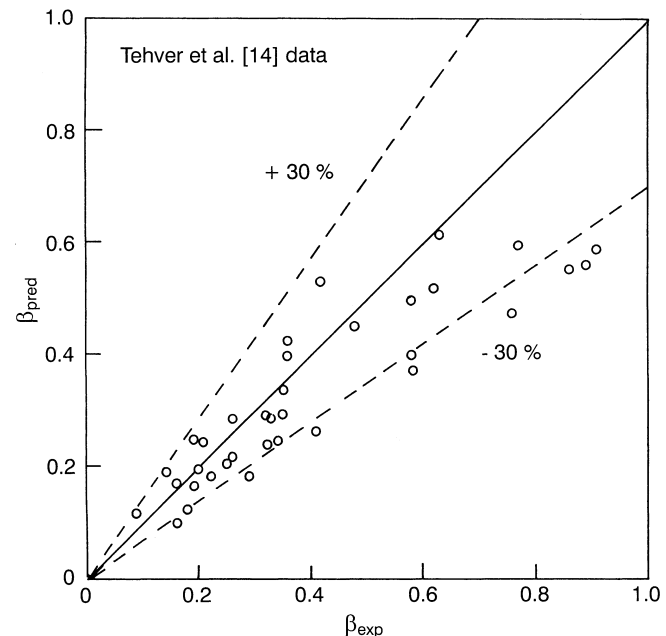


Fig. 7. Performance of the correlation for the nucleation factor, ' β '

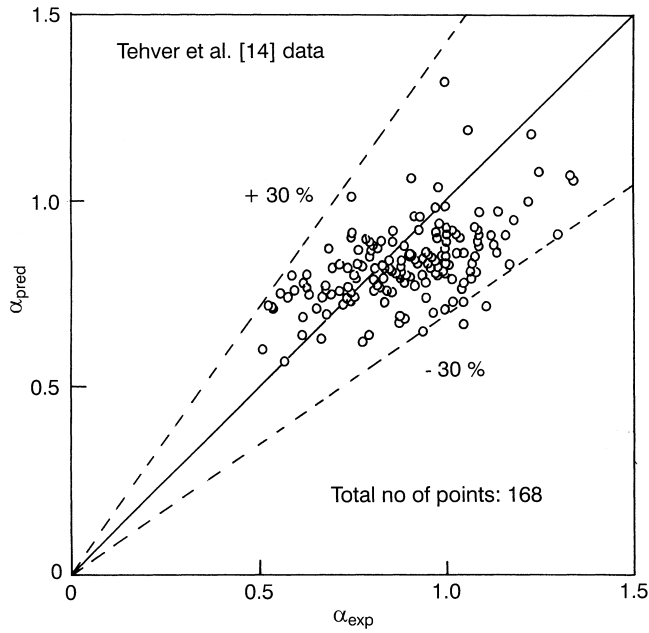


Fig. 8. Performance of the correlation for the nucleation factor, ' α '

$$q = 2.4 \times 10^{-4} \frac{\rho_l \rho_v^2 K \lambda^2 \Delta T (\delta/d)^{0.8} Ja^{0.22}}{\mu_v \delta T_s (\rho_l - \rho_v) \epsilon^{1.23}} \quad (20)$$

The above expression is compared with data available in the literature. The mean pore diameter ' d ' is required to use Eq. (20), but generally only the average particle diameter ' d_p ' is reported in the literature. Therefore, for comparison purposes, the mean pore diameter, ' d ' is approximated in terms of the average particle diameter by considering regular packing geometries. These approximations are shown in Table 2. The performance of the present model is shown in Fig. 9. The model fits the literature data very well. It may be noted that the data has been taken from four different sources. It includes pool boiling data over flat porous surfaces due to Styrikovich et al. [16] apart from the data of Tehver et al. [14]. The model also matches pool boiling data obtained over horizontal tubes with porous surfaces reported by Nishikawa et al. [10] and Afgan et al. [13]. This shows that curvature

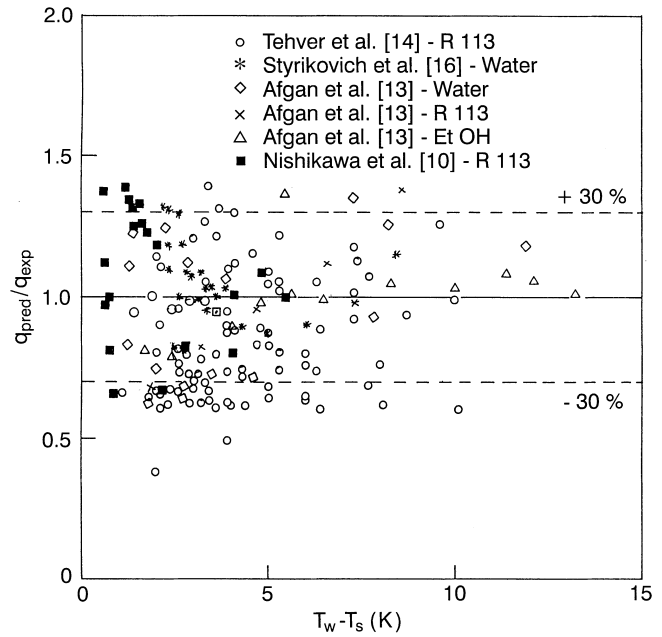


Fig. 9. Comparison of the present model with pool boiling data over porous surfaces from the literature

effects are not important in the pool boiling of liquids over porous surfaces as the model compares satisfactorily data obtained on flat surfaces as well as on horizontal tubes without any modifications. The liquids used in these studies include water, R 113 and ethanol. The total number of data points shown in Fig. 9 is 174.

It may be noted that the correlation of Nishikawa et al. [10] showed a very poor fit when compared to the data of Afgan et al. [13]. The expression developed in the present study shows that $q \propto \Delta T^{1.22}$. But the boiling data of Afgan et al. [13] shows that $q \propto \Delta T^n$, where n varies from 0.42 to 3.8 depending upon the mode of boiling and the surface liquid combination. However, in the present study, only data obtained in the bubble mode in the Afgan et al. [13] study was used for comparison purposes. Ayub and Bergles [17] proposed an empirical correlation for R 113 and water for boiling at 1.0 atmosphere on a GEWA-TW tube in which $q \propto \Delta T$ which is close to the present ex-

Table 2. Details of surface and liquid combinations from literature data used for comparison with present model

Sl. no	Source	Heating surface	Liquid	Particle dia. mean d_p , μm	Mean pore dia., d	No. of data points
1.	Tehver et al. [14]	aluminum and copper	R 113	not given	1–15.7 μm	93
2.	Afgan et al. [13]	Cr-Ni stainless steel tubes	water	81.5	0.414 d_p for $\epsilon < 0.4$ ϵd_p for $\epsilon = 0.7$	18
3.			R 113	81.5	0.2 d_p	7
4.			Ethanol	81.5	0.2 d_p	13
5.	Nishikawa et al. [10]	copper tube	R 113	250	0.2 d_p	21
6.	Styrikovich [16]	Nichrome	water	150	0.414 d_p	22

pression. However, it must be noted that the present approach is much more general and the range of variables much greater than the Ayub and Bergles [17] correlation.

4

Conclusions

The pressure drop across the porous boiling surface has to be carefully assessed by considering the Darcy's pressure drop and the equilibrium pressure difference for the bubbles to be able to exit from the surface. The slope of the vapour pressure curve has to be modified accordingly for the Clayperon's equation. The heat flux contribution due to single phase external convection is considerable when the surface porosity is small, but negligible for porous surfaces where surface porosity is high. The burnout heat flux for porous surfaces is purely a geometrical constraint. The nucleation site density at any heat flux has a definite relation with the maximum number of pores available for a given matrix geometry.

References

1. Thome, J. R.: Enhanced Boiling Heat Transfer. Washington D.C., U.S.A.: Hemisphere Publishing Corp. 1990
2. Stephan, K.: Heat Transfer in Condensation and Boiling. New York, Berlin: Springer-Verlag 1992
3. Webb, R. L.: Principles of Enhanced Heat Transfer. New York: John Wiley and Sons 1994
4. O'Neill, P. S.; Gottzmann, C. F.; Terbot, J. W.: Novel Heat Exchanger increases Cascade Cycle Efficiency for Natural Gas Liquefaction. Timmerhaus, K. D. (ed) Advances in Cryogenic Engineering Plenum, New York, 17 (1972) 420-437
5. Webb, R. L.: Nucleate Boiling on Porous Coated Surfaces. Heat Transfer Engineering 4 (1983) 71-82
6. Kovalev, S. A.; Solovyev, S. L.; Ovodkov, O. A.: Liquid Boiling on Porous Surfaces. Heat Transfer - Soviet Research. 19 (1987) 109-120
7. Kovalev, S. A.; Solovyev, S. L.; Ovodkov, O. A.: Theory of Boiling Heat Transfer on a Capillary Porous Surface. Proceedings 9th International Heat Transfer Conference, Jerusalem, Israel 2 (1990) 105-110
8. Nakayama, W.; Daikoku, T.; Kuwahara, H.; Nakajima, Y.: Dynamic Model of Enhanced Heat Transfer on Porous Surfaces - Part I. ASME Journal of Heat Transfer 102 (1980) 445-450
9. Nakayama, W.; Daikoku, T.; Kuwahara, H.; Nakajima, Y.: Dynamic Model of Enhanced Heat Transfer on Porous Surfaces - Part II. ASME Journal of Heat Transfer 102 (1980) 451-456
10. Nishikawa, K.; Ito, T.; Tanaka, K.: Augmented Heat Transfer by Nucleate Boiling at Prepared Surfaces. Proceedings ASME-JSME Thermal Engineering Conference 1 (1983) 387-393
11. Zhang, Y.; Zhang, H.: Boiling Heat Transfer from a Thin Powder Porous Layer at Low and Moderate Heat Flux. Chen, X. J.; Veziroglu, T. N.; Tien, C. L. (eds) Multiphase Flow and Heat Transfer, Second International Symposium, New York. Hemisphere Publishing Corp. (1992) 358-366
12. Bergles, A. E.; Chyu, M. C.: Characteristics of Nucleate Pool Boiling from Porous Metallic Coatings. Advances in Enhanced Heat Transfer. ASME HTD-18 (1981) 61-71
13. Afgan, N. H.; Jovic, L. A.; Kovalev, S. A.; Levykov, V. A.: Boiling Heat Transfer from Surfaces with Porous Layers. Int. J. Heat Transfer 28 (1985) 415-422
14. Tehver, J.; Sui, H.; Temkina, V.: Heat Transfer and Hysteresis Phenomena in Boiling on Porous Plasma Sprayed Surface. Exp. Thermal Fluid Sci. 5 (1992) 714-727
15. Kaviany, M.: Principles of Heat Transfer in Porous Media. New York: Springer Verlag 1991.
16. Styrikovich, M. A.; Malysenko, S. P.; Andrianov, A. B.; Talaev, L. V.: Investigation of Boiling on Porous Surfaces. Heat Transfer - Soviet Research. 19 (1987) 23-29
17. Ayub, Z. H.; Bergles, A. E.: Pool Boiling from GEWA Surfaces in Water and R-113. Wärme und Stoffübertragung 21 (1987) 209-219